

## Optimal paths in disordered media: Scaling of the crossover from self-similar to self-affine behavior

Markus Porto,<sup>1,2,\*</sup> Nehemia Schwartz,<sup>2</sup> Shlomo Havlin,<sup>2</sup> and Armin Bunde<sup>1</sup>

<sup>1</sup>*Institut für Theoretische Physik III, Justus-Liebig-Universität Giessen, Heinrich-Buff-Ring 16, 35392 Giessen, Germany*

<sup>2</sup>*Minerva Center and Department of Physics, Bar-Ilan University, 52900 Ramat-Gan, Israel*

(Received 28 June 1999)

We study optimal paths in disordered energy landscapes using energy distributions of the type  $P(\log_{10} E) = \text{const}$  that lead to the strong disorder limit. If we truncate the distribution, so that  $P(\log_{10} E) = \text{const}$  only for  $E_{\min} \leq E \leq E_{\max}$ , and  $P(\log_{10} E) = 0$  otherwise, we obtain a crossover from self-similar (strong disorder) to self-affine (moderate disorder) behavior at a path length  $\ell_{\times}$ . We find that  $\ell_{\times} \propto [\log_{10}(E_{\max}/E_{\min})]^{\kappa}$ , where the exponent  $\kappa$  has the value  $\kappa = 1.60 \pm 0.03$  both in  $d=2$  and  $d=3$ . We show how the crossover can be understood from the distribution of local energies on the optimal paths. [S1063-651X(99)51409-8]

PACS number(s): 05.40.-a, 02.50.-r, 64.60.Ak

The problem of finding and characterizing the optimal path in a disordered energy landscape has attracted much interest in recent years [1–9]. In many applications the energy landscape is rugged and optimization is crucial to find the global minimum path or configuration, which is dominating the low temperature behavior. Prominent examples of optimization problems include spin glasses [10], folding of proteins [11], and the well-known traveling salesman problem [12].

For an energy landscape on a directed lattice, the paths are self-affine and belong to the universality class of directed polymers (DP) (see, e.g., [5]). This universality class is characterized by fluctuations of the width of the path  $w(t)$  as a function of path length  $t$ , which scales as  $w(t) \sim t^{\alpha}$ . Here,  $\alpha$  is the DP roughness exponent, being  $2/3$  in  $1+1$  dimensions and  $0.62 \pm 0.01$  in  $2+1$  dimensions [5].

Recently, Cieplak *et al.* [6] considered optimal paths in isotropic systems in the strong disorder limit (sometimes also called the ultrametric limit). In this limit, the energies associated with the bonds of a given lattice are assumed to be drawn from a very broad distribution, such that the path between two points is dominated by the maximum barrier along it. In this case, the total energy of the path (which is the sum of all energies along the path) can be well approximated by this maximum barrier. Cieplak *et al.* [6] introduced a novel algorithm [13] and found that an optimal path in such an energy landscape is a fractal. The length  $\ell$  of the path scales with the end-to-end distance  $r$  as  $\ell \sim r^{d_{\text{opt}}}$  with  $d_{\text{opt}} = 1.22 \pm 0.01$  in  $d=2$ ,  $d_{\text{opt}} = 1.42 \pm 0.02$  in  $d=3$ , and  $d_{\text{opt}} = 1.59 \pm 0.02$  in  $d=4$ . For a moderate energy disorder, such as a uniform or Gaussian distribution, the isotropic case was studied recently by Schwartz *et al.* [9] applying Dijkstra's algorithm [14]. They find, for both  $d=2$  and  $d=3$ , that the path remains self-affine and within the universality class of DP.

The crossover from self-similar to self-affine behavior was first established in [15] for an Ising system in  $d=2$  with

random exchange strengths and antiperiodic boundary conditions. It was observed that, depending on the competition between the system size and broadness of the distribution of exchange strengths, a crossover from self-similar to self-affine behavior of the interface line between the two domains (i.e., of the optimal path) occurs. However, the scaling behavior of the crossover was not studied quantitatively, and it is not clear *how* the optimal path is changed when moving from one disorder limit to the other one. Here we study quantitatively the dependence of the nature of the disorder on the length of the optimal path considered. We show that some energy distributions can be regarded as “strong” on short length scales and “moderate” on large length scales, such that fractal behavior occurs below a characteristic length scale  $\ell_{\times}$  and self-affine behavior above it.

To better understand the relation between optimal path and strength of underlying disorder, we study the optimal path for energy distributions  $P(\log_{10} E) = \text{const}$  for  $E_{\min} \leq E \leq E_{\max}$  and  $P(\log_{10} E) = 0$  otherwise [16]. By changing the ratio  $E_{\max}/E_{\min}$  we can tune the degree of disorder. We find (in agreement with [15]) that the optimal path is self-similar at short length scales and self-affine at large length scales. The crossover length  $\ell_{\times}$  scales as  $\ell_{\times} \sim [\log_{10}(E_{\max}/E_{\min})]^{\kappa}$  where, surprisingly the exponent  $\kappa = 1.60 \pm 0.03$  does not seem to depend on the dimensionality of the system.

For detecting the optimal path we use Dijkstra's algorithm [14], which is valid as long as the energies  $E_i$  associated with the bonds are non-negative. We use square and simple cubic (sc) bond lattices with size  $L=2001$  in  $d=2$  and  $L=229$  in  $d=3$ , respectively. For the distribution of bond energies  $P(\log_{10} E) = \text{const}$  we find that the radius of gyration of the optimal path squared  $r^2(\ell)$  scales as  $r^2(\ell) \sim \ell^{2/d_{\text{opt}}}$  as a function of the path length  $\ell$ . The numerical results for  $r^2(\ell)$  vs  $\ell$  for both  $d=2$  and  $d=3$  are shown in Fig. 1. The obtained fractal dimensions  $d_{\text{opt}} = 1.22 \pm 0.02$  in  $d=2$  and  $d_{\text{opt}} = 1.43 \pm 0.03$  in  $d=3$  are in very good agreement with the values obtained earlier [6,17].

If we truncate the distribution at certain lower and upper bounds  $E_{\min}$  and  $E_{\max}$ , so that  $P(\log_{10} E) = \text{const}$  only for  $E_{\min} \leq E \leq E_{\max}$  and  $P(\log_{10} E) = 0$  otherwise, we find a

\*Present address: School of Chemistry, Tel Aviv University, 69978 Tel Aviv, Israel.

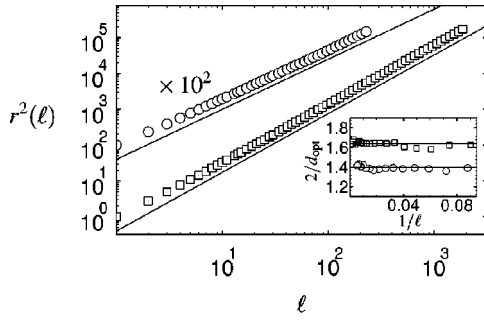


FIG. 1. Plot of the radius of gyration squared  $r^2(\ell)$  vs path length  $\ell$ , for  $d=2$  (open squares) and  $d=3$  (open circles, multiplied by  $10^2$ ). In both cases, a distribution of bond energies  $P(\log_{10} E) = \text{const}$  is used. The lines shown have a slope  $2/d_{\text{opt}} = 2/1.22$  ( $d=2$ ) and  $2/d_{\text{opt}} = 2/1.43$  ( $d=3$ ). The inset shows the local slopes vs  $1/\ell$ . The averages are performed on ensembles of  $10^4$  paths.

crossover from self-similar (characteristic of strong disorder) to self-affine (characteristic of moderate disorder) behavior at a path length  $\ell_{\times}$  (see Fig. 2). For  $\ell < \ell_{\times}$  the path shows self-similar behavior as before, i.e., the radius of gyration squared behaves as  $r^2(\ell) \sim \ell^{2d_{\text{opt}}}$  with the known fractal dimension  $d_{\text{opt}}$ , and the fluctuation of the width squared shows the behavior  $w^2(t) \sim t^2$ , as expected for self-similar structures. At the length  $\ell_{\times}$  the highest energy loses the ability to dominate the optimal path and the behavior changes drastically; for  $\ell > \ell_{\times}$  the path is no longer self-

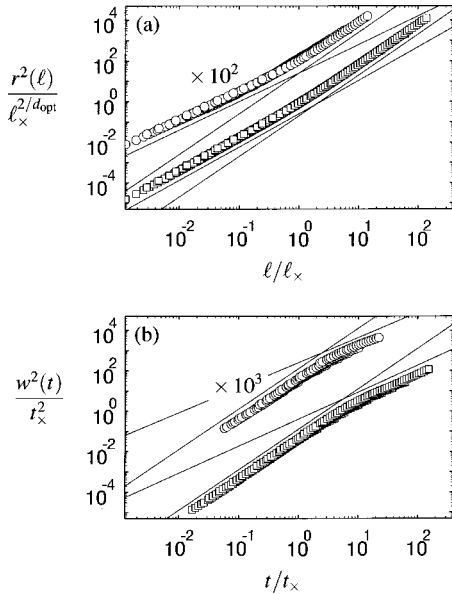


FIG. 2. (a) Scaling plot of the radius of gyration squared  $r^2(\ell)/\ell^{2/d_{\text{opt}}}$  vs  $\ell/\ell_{\times}$  with  $\ell_{\times} = [\log_{10}(E_{\text{max}}/E_{\text{min}})]^{\kappa}$ , for  $d=2$  (open squares) and  $d=3$  (open circles, multiplied by  $10^2$ ). The lines shown have slopes  $2/d_{\text{opt}} = 2/1.22$  and  $2$  ( $d=2$ ), and  $2/d_{\text{opt}} = 2/1.43$  and  $2$  ( $d=3$ ). (b) Scaling plot of the fluctuation of width squared  $w^2(t)/t_{\times}^2$  vs  $t/t_{\times}$  with  $t_{\times} = [\log_{10}(E_{\text{max}}/E_{\text{min}})]^{\kappa/d_{\text{opt}}}$ , for  $d=2$  (open squares) and  $d=3$  (open circles, multiplied by  $10^3$ ). The transient regimes with  $t \leq 6$  ( $d=2$ ) and  $t \leq 9$  ( $d=3$ ) are removed for clarity. The lines shown have a slope  $2$  and  $2\alpha = 4/3$  ( $d=2$ ), and  $2$  and  $2\alpha = 1.24$  ( $d=3$ ). In all four cases,  $\kappa = 1.6$  and  $\log_{10}(E_{\text{max}}/E_{\text{min}}) = 3.75, 7.5, 11, 16, 23, 32, 45, 60,$  and  $100$  are used. The averages are performed over  $10^4$  paths.

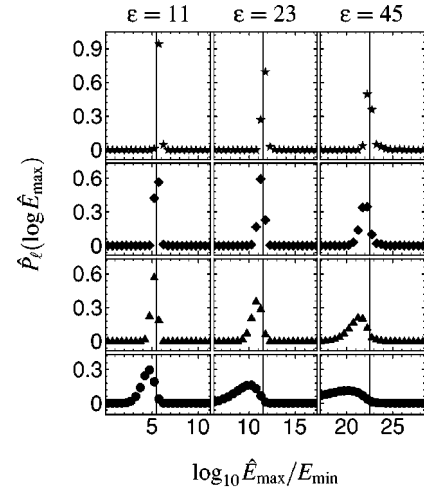


FIG. 3. Plot of the distribution of the maximum energy  $\hat{P}_{\ell}(\log_{10} \hat{E}_{\text{max}})$  vs  $\hat{E}_{\text{max}}/E_{\text{min}}$  in  $d=2$  for different truncations  $\varepsilon \equiv \log_{10}(E_{\text{max}}/E_{\text{min}}) = 11, 23,$  and  $45$  (from left to right) and different path lengths  $\ell = 9$  (full circles),  $49$  (full triangles),  $199$  (full diamonds), and  $999$  (full stars) (from bottom to top). The vertical lines indicate the respective critical energy  $\log_{10}(E_c/E_{\text{min}}) = p_c \log_{10}(E_{\text{max}}/E_{\text{min}})$  [18]. The averages are performed on ensembles of  $10^4$  paths.

similar but shows self-affine behavior, i.e., the radius of gyration squared crosses over to the trivial behavior  $r^2(\ell) \sim \ell^2$ , and the fluctuation of the width squared behaves now as  $w^2(t) \sim t^{2\alpha}$ , where  $\alpha$  is the same as the exponent for directed polymers. For the crossover length  $\ell_{\times}$  we obtain a scaling  $\ell_{\times} \propto [\log_{10}(E_{\text{max}}/E_{\text{min}})]^{\kappa}$ , where the exponent  $\kappa$  has the value  $\kappa = 1.60 \pm 0.03$  both in  $d=2$  and  $d=3$  and may therefore be independent of dimension.

Since  $\ell_{\times}$  is the only relevant length scale, we expect that  $r^2(\ell) = \ell_{\times}^{2d_{\text{opt}}} f(\ell/\ell_{\times})$  and  $w^2(t) = t_{\times}^2 g(t/t_{\times})$  with  $t_{\times} \sim \ell_{\times}^{1/d_{\text{opt}}}$  and two scaling functions  $f(x)$  and  $g(x)$ . In Fig. 2(a) we show a data collapse for  $r^2(\ell)$  when plotting  $r^2(\ell)/\ell_{\times}^{2d_{\text{opt}}}$  vs  $\ell/\ell_{\times}$  for  $\log_{10}(E_{\text{max}}/E_{\text{min}})$ , ranging from  $3.75$  to  $100$ , supporting the scaling in  $d=2$  and  $d=3$ . For the second quantity of interest  $w^2(t)$ , a similar data collapse can be obtained by plotting  $w^2(t)/t_{\times}^2$  vs  $t/t_{\times}$ , as done in Fig. 2(b). For both  $r^2(\ell)$  and  $w^2(t)$  we obtain very good data collapse. For the system size  $L_{\times}$ , at which the crossover occurs, follows  $L_{\times} \sim \ell_{\times}^{1/d_{\text{opt}}} \propto [\log_{10}(E_{\text{max}}/E_{\text{min}})]^{\kappa/d_{\text{opt}}}$ , with  $\kappa/d_{\text{opt}} \approx 1.31$  in  $d=2$  and  $\kappa/d_{\text{opt}} \approx 1.12$  in  $d=3$ .

To achieve a better understanding of the crossover, we study the energy distribution on the generated optimal paths. Since we expect the maximum energy  $\hat{E}_{\text{max}}$  on a path of length  $\ell$  to be the key quantity determining the crossover, we focus here on the distribution of these maximum energies  $\hat{P}_{\ell}(\log_{10} \hat{E}_{\text{max}})$  on paths of length  $\ell$ . As an example, we present numerical results for  $d=2$  in Fig. 3, where we show  $\hat{P}_{\ell}(\log_{10} \hat{E}_{\text{max}})$  for three different energy truncations  $\varepsilon \equiv \log_{10}(E_{\text{max}}/E_{\text{min}}) = 11, 23,$  and  $45$  (in these cases  $\ell_{\times} \approx 46, 150,$  and  $440$ ) and four different path lengths  $\ell = 9, 49, 199,$  and  $999$ . The results can be summarized as follows: the distributions are bell shaped, as the path length  $\ell$  increases they get narrower, and the positions of their maxima shift towards higher energies. Close to  $\ell_{\times}$  the distributions become very

narrow peaks at the respective critical energy  $\log_{10}(E_c/E_{\min})=p_c \log_{10}(E_{\max}/E_{\min})$  [18], where  $p_c$  is the critical concentration of the respective lattice [ $p_c=1/2$  for the bond square lattice in  $d=2$  and  $p_c \cong 0.248814$  for the bond sc lattice in  $d=3$  (see, e.g., [19]). For  $\ell > \ell_\times$ , the distributions remain as narrow peaks at the respective critical energy  $E_c$ .

For a more quantitative measure of the observations described above, one possible quantity to study is the cumulative probability that accumulates *around* the respective critical energy. One expects this measure to be small for  $\ell \ll \ell_\times$ , reflecting the fact that there are only very few high energy bonds on the path, such that a single one is able to dominate the path's behavior and the system is in the strong disorder limit. The measure is expected to increase with  $\ell$  until reaching the value 1 for  $\ell \gg \ell_\times$ , resembling the loss of ability of a single bond to control the path, yielding the limit of moderate disorder. Formally, we define

$$\Pi_\varepsilon(\ell) \equiv \int_{\log_{10}[E_c(\varepsilon)] - \hat{\varepsilon}}^{\infty} \hat{P}_\ell(\log_{10} \hat{E}_{\max}) d(\log_{10} \hat{E}_{\max}), \quad (1)$$

with an arbitrary small  $\hat{\varepsilon} > 0$  as the cumulative probability around the respective critical energy  $E_c(\varepsilon)$  for a given  $\varepsilon \equiv \log_{10}(E_{\max}/E_{\min})$ . As an example, we show in Fig. 4(a) a scaling plot  $\Pi_\varepsilon(\ell)$  vs  $\ell/\ell_\times$  for ten values of  $\varepsilon$  ranging from  $\varepsilon=11$  to 54 in  $d=2$ . It can be seen that the data collapses quite nicely on a single curve, so that  $\Pi_\varepsilon(\ell)$  is only a function of the combined variable  $\ell/\ell_\times$ . In addition, it can be seen that  $\Pi_\varepsilon(\ell) \propto \ell/\ell_\times$  for  $\ell/\ell_\times < 1$  and that the crossover occurs roughly where  $\Pi_\varepsilon(\ell_\times) = \Pi_\times$  with  $\Pi_\times \cong 0.2$ . [The value  $\Pi_\times \cong 0.2$  of course depends on the choice of  $\hat{\varepsilon}$  (in our case  $\hat{\varepsilon}=0.05$ ), but the qualitative behavior of  $\Pi_\varepsilon(\ell_\times)$  is independent of  $\hat{\varepsilon}$ .] The structure belongs to the universality class of the optimal path in strong disorder as long as the probability  $\Pi_\varepsilon(\ell)$  [which is the probability of having a maximum energy approximately equal to the critical energy  $E_c(\varepsilon)$  on a path of this length] is smaller than  $\Pi_\times$ . The crossover occurs at a path length  $\ell_\times$ , where this cumulative probability becomes equal to  $\Pi_\times$ . For  $\ell > \ell_\times$  the maximum energy occurs too frequently and hence there is no longer a single energy that is able to dominate the path's behavior. As a result, we recover the universality class of the directed polymer problem.

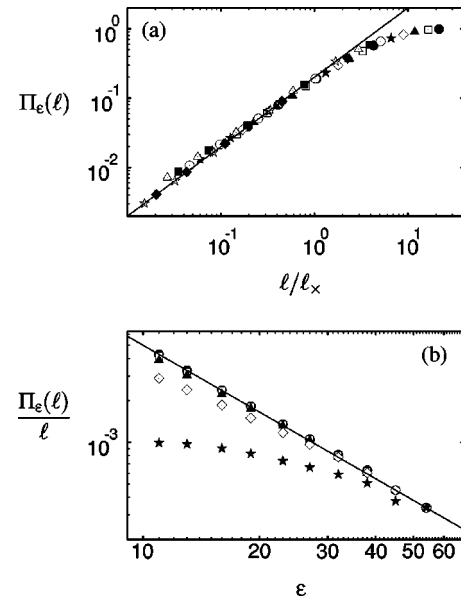


FIG. 4. (a) Scaling plot of the cumulative probability  $\Pi_\varepsilon(\ell)$  vs  $\ell/\ell_\times$  with  $\ell_\times = [\log_{10}(E_{\max}/E_{\min})]^\kappa$  in  $d=2$  for different truncations  $\varepsilon \equiv \log_{10}(E_{\max}/E_{\min})=11$  (full circles), 13 (open squares), 16 (full triangles), 19 (open diamonds), 23 (full stars), 27 (open circles), 32 (full squares), 38 (open triangles), 45 (full diamonds), and 54 (open stars), and  $\kappa=1.6$ . The line shown has a slope 1. (b) Scaling plot of  $\Pi_\varepsilon(\ell)/\ell$  vs  $\varepsilon$  for  $\ell=9$  (full circles), 19 (open squares), 49 (full triangles), 199 (open diamonds), and 999 (full stars). The line shown has a slope  $-1.6 \cong -\kappa$ . For the numerical integration a value of  $\hat{\varepsilon}=0.05$  is used and the averages are performed on ensembles of  $10^4$  paths.

From the quantity  $\Pi_\varepsilon(\ell)$  one is also able to deduce the scaling of the crossover length  $\ell_\times$ . Since  $\Pi_\varepsilon(\ell) \propto \ell/\ell_\times$  for  $\ell < \ell_\times$ , it follows that  $\Pi_\varepsilon(\ell) = \Pi_0 \ell \varepsilon^{-\kappa}$  in this regime, so that  $\Pi_\varepsilon(\ell)/\ell$  is a constant for fixed  $\varepsilon$  and scales as  $\Pi_\varepsilon(\ell)/\ell \propto \varepsilon^{-\kappa}$ , which can be seen in Fig. 4(b). This means that the crossover and its scaling behavior can be described by the distribution of maximum energies  $\hat{P}_\ell(\log_{10} \hat{E}_{\max})$  on the path and its related quantity  $\Pi_\varepsilon(\ell)$ . The fact that dimensionality is explicitly neither involved in  $\hat{P}_\ell(\log_{10} \hat{E}_{\max})$  nor in  $\Pi_\varepsilon(\ell)$  further supports the possibility that  $\kappa = 1.60 \pm 0.03$  is independent of dimension.

This work has been supported by the Deutsche Forschungsgemeinschaft, the Minerva Center for the Physics of Mesoscopics, Fractals and Neural Networks, and the German-Israeli Foundation.

- [1] D.A. Huse and C.L. Henley, Phys. Rev. Lett. **54**, 2708 (1985); M. Kardar, *ibid.* **55**, 2923 (1985); D.A. Huse, C.L. Henley, and D.S. Fisher, *ibid.* **55**, 2924 (1985).
- [2] M. Kardar, G. Parisi, and Y.-C. Zhang, Phys. Rev. Lett. **56**, 889 (1986); M. Kardar and Y.-C. Zhang, *ibid.* **58**, 2087 (1987).
- [3] E. Perlsman and M. Schwartz, Europhys. Lett. **17**, 11 (1992); M. Schwartz and S.F. Edwards, *ibid.* **20**, 301 (1992); E. Perlsman and M. Schwartz, Physica A **234**, 523 (1996).
- [4] T. Halpin-Healy and Y.-C. Zhang, Phys. Rep. **254**, 215 (1995).
- [5] A.-L. Barabási and H.E. Stanley, *Fractal Concepts in Surface*

*Growth* (Cambridge University Press, Cambridge, England, 1995), and references therein.

- [6] M. Cieplak, A. Maritan, and J.R. Banavar, Phys. Rev. Lett. **72**, 2320 (1994); **76**, 3754 (1996).
- [7] A.-L. Barabási, Phys. Rev. Lett. **76**, 3750 (1996).
- [8] P. De Los Rios and Y.-C. Zhang, Phys. Rev. Lett. **81**, 1023 (1998).
- [9] N. Schwartz, A. Nazaryev, and S. Havlin, Phys. Rev. E **58**, 7642 (1998).
- [10] M. Mezard, G. Parisi, N. Sourlas, G. Toulouse, and M. Virasoro,

- oro, Phys. Rev. Lett. **52**, 1156 (1984).
- [11] A. Ansari, J. Berendzen, S.F. Bowne, H. Fraunfelder, I.E.T. Iben, T.B. Sauke, E. Shyamsunder, and R.D. Young, Proc. Natl. Acad. Sci. USA **82**, 5000 (1985).
- [12] S. Kirkpatrick and G. Toulouse, J. Phys. (France) Lett. **46**, 1277 (1985).
- [13] In the strong disorder limit, the optimal path can be constructed in good approximation by ranking the energy values and removing the bonds according to their rank (starting with the highest energy value) until a single path remains. There is one constraint; if the removal of a bond will disconnect the two opposite faces of the lattice, the bond is not removed and one proceeds with the next bond in the rank list.
- [14] T.H. Cormen, C.E. Leiserson, and R.L. Rivest, *Introduction to Algorithms* (MIT Press, Cambridge, 1990).
- [15] M. Cieplak, A. Maritan, M.R. Swift, A. Bhattacharya, A.L. Stella, and J.R. Banavar, J. Phys. A **28**, 5693 (1995).
- [16] This energy distribution is similar to the distribution of exchange strengths studied in [15]. The choice of  $P(\log_{10}E) = \text{const}$  as distribution of energies is motivated by the following considerations. For the occurrence of strong disorder, high energies need to be frequent enough so that they are present in the system, but also rare enough so that they are able to govern the total energy of the path. If high energies are too less probable compared to low energies, they can be easily avoided by the optimization and will not be part of the optimal path. If high energies are too probable compared to low energies, the optimal path will contain many high energy bonds with similar values and a single one can no longer dominate.
- [17] M. Porto, S. Havlin, S. Schwarzer, and A. Bunde, Phys. Rev. Lett. **79**, 4060 (1997).
- [18] According to the critical path argument, a path of infinite length contains only energies below the critical energy  $E_c$  (i.e., the distribution of energies on the path  $\hat{P}(E)$  is truncated at  $E_c$ , so that  $\hat{P}(E) > 0$  only for  $E_{\min} \leq E \leq E_c$ , and  $\hat{P}(E) = 0$  for  $E_c < E \leq E_{\max}$ ). The critical energy  $E_c$  is, in general terms, given by  $\int_0^{E_c} P(E) dE = p_c$ , where  $P(E)$  is the distribution of energies and  $p_c$  is the critical concentration of the given lattice. For a distribution  $P(\log_{10} E) = \text{const}$  for  $E_{\min} \leq E \leq E_{\max}$  and  $P(\log_{10} E) = 0$  otherwise this reduces to  $\log_{10}(E_c/E_{\min}) = p_c \log_{10}(E_{\max}/E_{\min})$ .
- [19] *Fractals and Disordered Systems*, edited by A. Bunde and S. Havlin, 2nd ed. (Springer, Berlin, 1996); D. Stauffer and A. Aharony, *An Introduction to Percolation Theory*, 2nd ed. (Taylor & Francis, London, 1992); M. Sahimi, *Applications of Percolation Theory* (Taylor & Francis, London, 1994).